



Imaging and Sizing of Single DNA Molecules on a Mobile Phone

Qingshan Wei,^{†,‡,§} Wei Luo,[†] Samuel Chiang,^{†,⊥} Tara Kappel,^{†,||} Crystal Mejia,[†] Derek Tseng,[†] Raymond Yan Lok Chan,[†] Eddie Yan,[†] Hangfei Qi,[#] Faizan Shabbir,[†] Haydar Ozkan,[†] Steve Feng,[†] and Aydogan Ozcan^{*,†,‡,§,▽}

[†]Electrical Engineering Department, University of California, Los Angeles, California 90095, United States, [‡]Bioengineering Department, University of California, Los Angeles, California 90095, United States, [§]California NanoSystems Institute (CNSI), University of California, Los Angeles, California 90095, United States, [⊥]Department of Chemistry and Biochemistry, University of California, Los Angeles, California 90095, United States, ^{||}Department of Neurobiology, University of California, Los Angeles, California 90095, United States, [#]Department of Molecular and Medical Pharmacology, University of California, Los Angeles, California 90095, United States, and [▽]Department of Surgery, University of California, Los Angeles, California 90095, United States

ABSTRACT DNA imaging techniques using optical microscopy have found numerous applications in biology, chemistry and physics and are based on relatively expensive, bulky and complicated set-ups that limit their use to advanced laboratory settings. Here we demonstrate imaging and length quantification of single molecule DNA strands using a compact, lightweight and cost-effective fluorescence microscope installed on a mobile phone. In addition to an optomechanical attachment that creates a high contrast dark-field imaging setup using an external lens, thin-film interference filters, a miniature dovetail stage and a laser-diode for oblique-angle excitation, we also created a computational framework and a mobile phone application connected to a server back-end for measurement of the lengths of individual DNA molecules that are labeled and stretched using disposable chips. Using this mobile phone platform, we imaged single DNA molecules of various lengths to demonstrate a sizing accuracy of <1 kilobase-pairs (kbp) for 10 kbp and longer DNA samples imaged over a field-of-view of $\sim 2 \text{ mm}^2$.



KEYWORDS: cell phone microscopy · fluorescence imaging · DNA imaging · DNA sizing · point-of-care · mobile health

Optical methods for imaging single biomolecules allow for exploration of their individual behavior and properties at nanoscale, which not only significantly advance our knowledge of molecular biology and biophysics but also provide various diagnostics opportunities for biomedical applications.^{1–13} Imaging of single DNA molecules has been of particular interest as various diseases including cancer and neurological disorders such as Alzheimer's disease are associated with genomic alterations, including for example copy-number variations (CNVs).^{14,15} High spatial resolution and nondestructive nature of optical imaging methods are especially attractive for probing DNA–protein interactions¹⁶ or mapping genetic information from individual DNA molecules.¹⁷ These research and development efforts, however, have been mostly limited to advanced laboratory facilities using relatively costly,

complex and bulky imaging set-ups, including for example confocal fluorescence microscopy,¹⁸ super-resolution microscopy,¹⁹ or label-free plasmonic imaging.²⁰ Translation of these and other existing imaging techniques to field-portable, cost-effective and high-throughput instruments would open up a myriad of new applications in, e.g., point-of-care (POC) medicine, global health and diagnostics fields, among others, and would also positively impact research and educational efforts in developing countries and resource-limited institutions, helping the democratization of advanced scientific instruments and measurement tools.²¹ For this broad aim, mobile phones and other consumer electronics devices, including, e.g., tablet PCs and wearable computers, have been emerging as powerful platforms to create cost-effective, portable and readily accessible alternatives to some of the advanced biomedical imaging and

* Address correspondence to ozcan@ucla.edu.

Received for review October 12, 2014 and accepted December 10, 2014.

Published online December 10, 2014
10.1021/nn505821y

© 2014 American Chemical Society

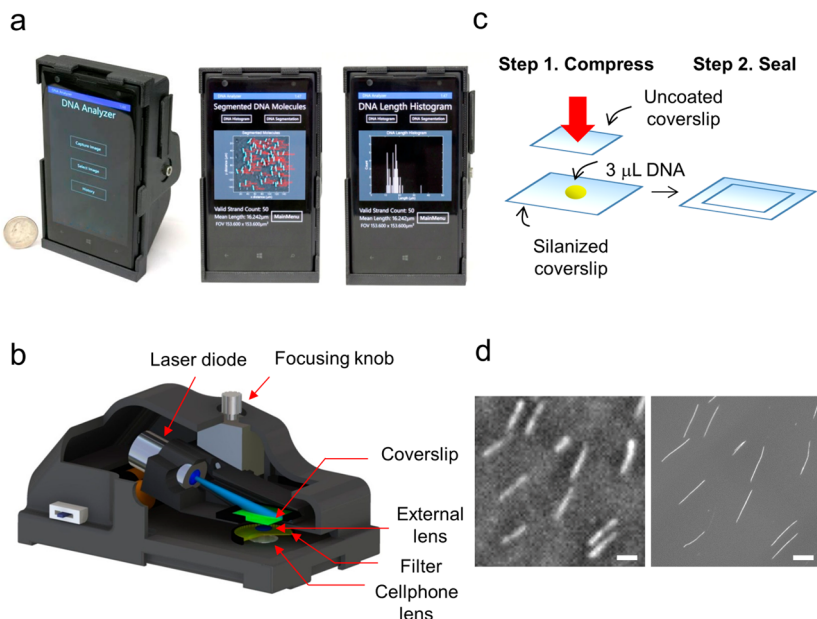


Figure 1. Imaging and sizing of single DNA molecules on a mobile phone. (a) Photographs of the mobile phone based fluorescence microscopy platform for single DNA molecule imaging and sizing. We also created a Windows-based smart application running on the same mobile phone that can transfer images from the phone to a custom-designed remote server and display the received DNA analysis results back on the screen of the phone. More screenshots of the same application are also provided in Figure S5. (b) A 3D AutoCAD illustration of the same optomechanical attachment. (c) Schematic illustration of a simple DNA stretching method used in this work. (d) Representative fluorescence microscope images of stretched λ DNA molecules that are acquired by using our mobile phone microscope (left) and a benchtop fluorescence microscope with a $100\times$ oil-immersion objective lens, NA = 1.3 (right). Scale bar, $10\ \mu\text{m}$.

measurement tools.^{22–30} Especially mobile phones have been experiencing massive advances in their optical imaging hardware, approximately doubling their space-bandwidth product every two years over the last \sim 10–15 years, recently reaching to more than 40 million pixels in their digital camera systems. In addition to their advanced optical interface, the computational power (now also including Graphics Processing Units, GPUs), data connectivity, massive volume (with >7 billion subscribers) and cost-effectiveness of mobile phones make them an ideal platform for conducting various advanced biomedical experiments and tests, including, e.g., blood analysis, measurement of analytes in bodily fluids, flow-cytometry, among various others.^{21,31–44} Despite all of these recent advances and progress, imaging of single DNA molecules on a mobile phone device could not be achieved until this work, leaving it as one of the major remaining milestones in mobile phone based imaging and micro-analysis systems, mostly due to extremely weak signal-to-noise ratio (SNR) and limited contrast of single molecule samples in optical part of the electro-magnetic spectrum.

In this article, we report the first demonstration of mobile phone based imaging and length quantification of individual DNA molecules using a field-portable and cost-effective optomechanical attachment that is created with additive manufacturing and integrated onto the existing camera module of a smart-phone (Figure 1a,b). This mobile microscopy unit, which

weighs less than 190 g (including three AAA batteries), utilizes a compact laser-diode (450 nm, 75 mW) to excite fluorescently labeled molecules at a high-incidence angle of $\sim 75^\circ$. When combined with thin-film based interference filters, this module creates a very strong dark-field performance, significantly suppressing the background noise created by the high-power excitation beam (Figure 1b). The same optomechanical unit also contains a miniature dovetail stage for depth-of-focus adjustment and an external lens (taken from another mobile phone camera) forming a magnified image of the fluorescent specimen onto the CMOS sensor-chip of the phone (Figure 1b). This lightweight attachment to the mobile phone, including all of its parts, costs approximately \$400, which is significantly cheaper than a conventional benchtop fluorescence microscope; furthermore, the cost can be considerably reduced with large volume manufacturing. In addition to this compact and cost-effective fluorescent microscope unit, we have also created a computational interface that is composed of a Windows-based mobile application (Figure 1a) running on the same phone for communication of our raw images with a custom-designed back-end server application for digital processing of the acquired fluorescent images to rapidly quantify the length of each DNA strand by fitting the cellphone microscope's two-dimensional (2D) point-spread-function (PSF) to the measured fluorescent signatures. The results of this DNA detection and length measurement process can be visualized both

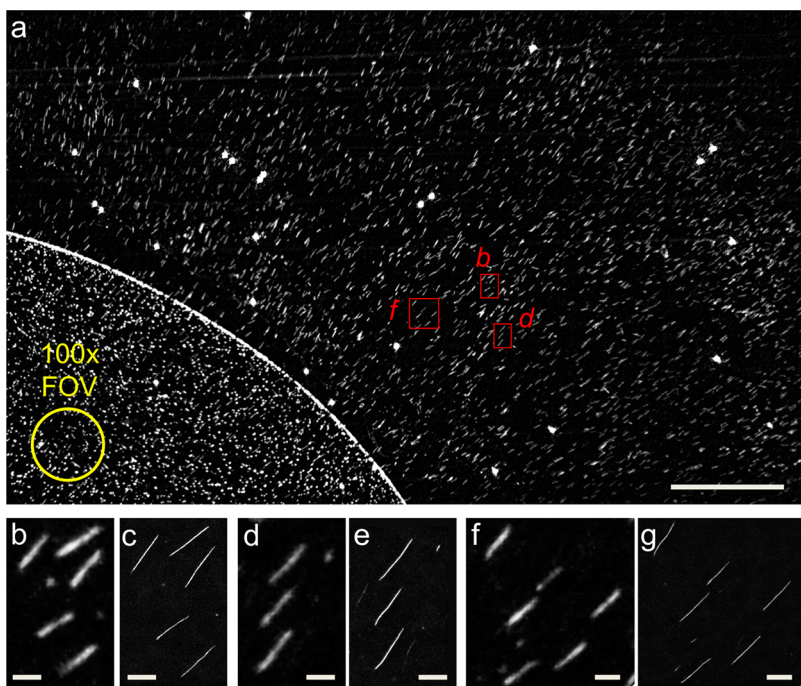


Figure 2. Fluorescence microscopy of stretched DNA molecules on a mobile phone. (a) Large FOV ($\sim 2 \text{ mm}^2$) mobile phone image of labeled DNA molecules stretched on a glass substrate. This image is taken at the boundary of the initial DNA droplet placed on the substrate, and it is averaged using 13 successive cellphone images and is displayed after background subtraction. Inset shows a typical FOV corresponding to a $100\times$ objective-lens. The large circular fluorescent spots that appear in this image are 500 nm green fluorescent polystyrene beads which are added into the sample to assist depth focusing and location matching (for comparison purposes). (b,d,f) Enlarged cellphone images showing single DNA molecules within the red boxes in (a). (c,e,g) Corresponding conventional benchtop fluorescence microscope images of the same molecules obtained using a $100\times$ oil-immersion objective lens (NA = 1.3) and a cooled monochrome CCD camera. Scale bar, 250 μm for (a) and 10 μm for (b–g).

at the mobile phone screen as well as through remote PCs (Figure 1a and Figure S5, Supporting Information).

We experimentally demonstrated the success of this mobile phone based DNA imaging and sizing platform using short DNA fragments with different lengths (5, 10, and 20 kbp) and relatively long bacteriophage DNA strands (λ and T7 DNA, 40 and 48 kbp, respectively), which were fluorescently labeled and linearly stretched using disposable chips, helping us achieve a length measurement accuracy of <1 kbp for 10 kbp and longer DNA molecules, imaged on the mobile phone over a large field-of-view of $\sim 2 \text{ mm}^2$. We should emphasize that this level of length measurement accuracy and throughput are sufficient for probing gene-level structure information from single DNA molecules, and therefore this platform can serve as the stepping stone for next-generation mobile biomedical analysis, sensing and diagnostic tools, and might potentially be used in various applications including, e.g., field and POC measurements of CNVs in human genome, early detection of cancers,⁴⁵ nervous system disorders⁴⁶ or drug resistance in infectious diseases such as malaria.⁴⁷

RESULTS AND DISCUSSION

In our experiments, mechanical stretching of DNA molecules from coiled form into a linear shape is achieved by quickly compressing a droplet of stained

DNA solution (3 μL) in between two coverslips to generate a transient fluid flow (Figure 1c).⁴⁸ This simple procedure stretches the DNA fragments by utilizing the strong shear force that is created at the silanized bottom glass substrate (for details refer to our Methods section and Supporting Information). The boundary of a DNA droplet can be observed at the center of the bottom coverslip after stretching, which is due to the adsorption of concentrated nonstretched DNA molecules at the liquid–air interface on the bottom coverslip. When compressed, DNA molecules were only stretched within the region outside the droplet boundary and remained nonstretched inside (see Figure 2a). This region of high-quality DNA stretching typically spans over a few millimeters away from the droplet boundary, which provides a sufficient sample area for imaging of DNA molecules using our mobile phone attachment over a large FOV of $\sim 2 \text{ mm}^2$. Figure 1d shows typical fluorescence images of individual DNA molecules that are stretched by using this method and imaged with our mobile phone based microscope as well as a benchtop microscope having a $100\times$ oil-immersion objective lens (Numerical Aperture, NA = 1.3) and a cooled monochrome CCD camera (see Supporting Information for details).

To test single DNA molecule imaging performance of our mobile phone microscope, we initially used

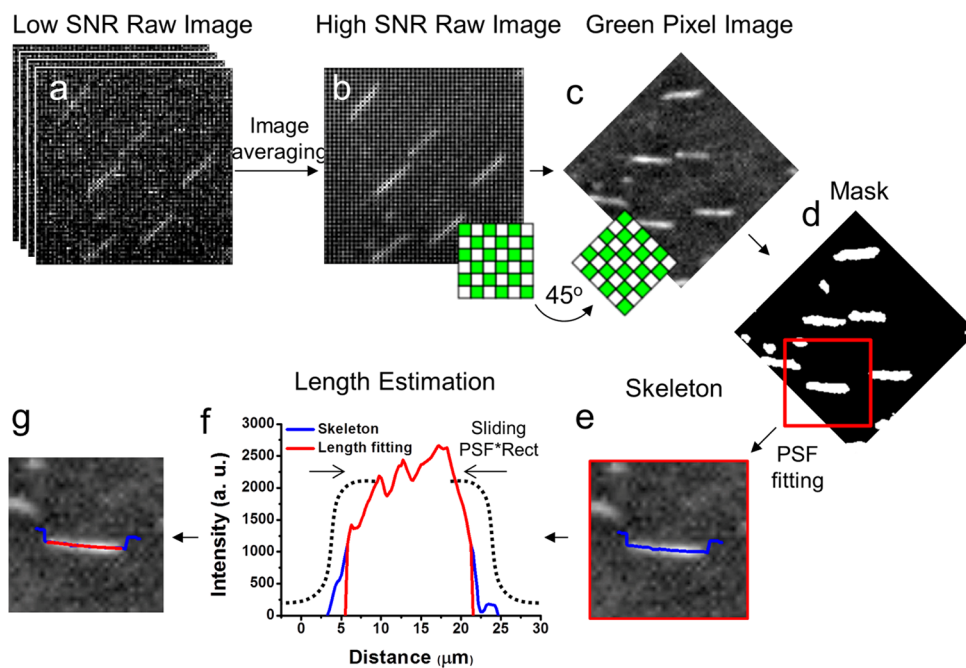


Figure 3. Flow-chart of automated DNA length quantification algorithm. (a) Sequence of mobile phone images of single DNA molecules, captured in DNG format. (b) High SNR mobile phone image obtained by averaging of the sequence in (a). (c) Formation of a green pixel only image by elimination of the blue and red pixels from the Bayer pattern in (b). Inset shows the rotation and rearrangement of the remaining green pixels. (d) Object mask generation step (also see Figure S3). (e) Superposition of the calculated skeleton (blue line) on a single DNA image taken from the red square in (d). (f) DNA length estimation through minimization of the difference between the actual measured edge intensity (blue line) and the theoretical edge function (dashed line, which is calculated by using one-dimensional convolution of the cellphone PSF with an ideal rectangular function). * denotes spatial convolution operation. (g) Estimated DNA length (red line) is superimposed onto the calculated DNA skeleton (blue line) and its mobile phone based fluorescence image.

double-stranded λ bacteriophage DNA (~ 48 kbp). The sample glass substrate with combed DNA molecules of interest (as illustrated in Figure 1c) was placed within our sample holder and inserted into the cellphone attachment. Image acquisition for each sample was repeated 10–15 times for the same region of interest with an exposure time of ~ 4 s per frame; these multiple frames were then averaged to create the final raw fluorescence image of the sample. Figure 2a displays one of these fluorescence images captured on our mobile phone device, showing that λ DNA molecules are linearly stretched around the initial droplet position and that the DNA alignment direction is approximately perpendicular to the boundary of the droplet. The cellphone image in Figure 2a covers a large FOV of $1.76\text{ mm} \times 1.09\text{ mm}$, and this is especially advantageous for high-throughput imaging and sizing of a large number of DNA molecules within the same sample. Figure 2b,d,f show some of the zoomed-in regions that are denoted with the red rectangles in Figure 2a, which clearly illustrate that the single DNA strands imaged on our mobile phone attachment exhibit a comparable contrast to the images of the same molecules obtained using a $100\times$ oil-immersion objective lens (NA = 1.30) and a passively cooled monochrome CCD camera on a conventional benchtop fluorescence microscope (Figure 2c,e,g).

To measure the lengths of individual DNA molecules imaged on our mobile phone based fluorescence microscopy platform, we created an algorithm which is summarized in Figure 3. This automated length estimation process starts with digital alignment and then averaging of multiple fluorescence images recorded on our mobile phone using the lossless digital negative (DNG) format,⁴⁹ which displays the image in a Bayer pattern⁵⁰ without any demosaicing and compression steps (Figure 3a,b). This averaging step significantly improves the SNR of our images; for example the mean SNR of single DNA molecules (calculated for over >350 individual DNA strands) increased from 3.8 for a single frame to an SNR of 12.1 for an average of 10 frames (see Figures S1 and S2), following an SNR improvement factor that is proportional to the square root of the number of frames (n). In our experiments we typically averaged 10–15 successive frames to benefit from this SNR improvement before the effects of photobleaching were observed. The second step in our length estimation framework involves rejection of all the blue and red pixels in the Bayer pattern such that only the green pixels of the image are kept, improving the spectral overlap with the fluorescent signal band (Figure 3c). The resulting green pixel array is then rotated by 45° to form a new image where the pixel period is “effectively” increased by $\sqrt{2}$ compared to the raw image pixel pitch; this is entirely due to the

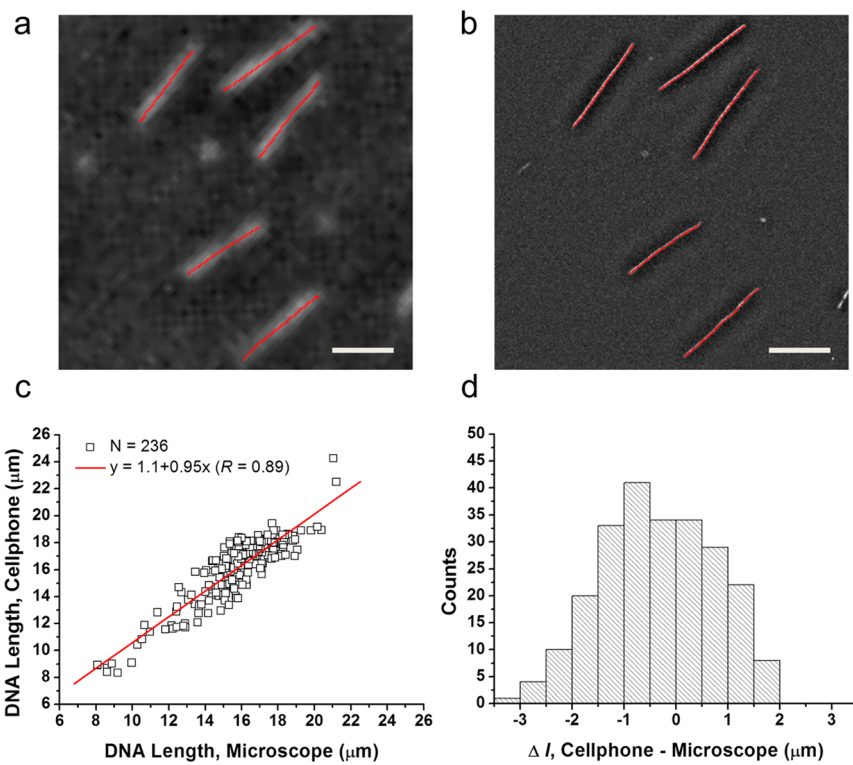


Figure 4. DNA length measurements. (a,b) Single λ DNA molecules imaged by our mobile phone device as well as a conventional benchtop microscope ($100\times$ oil-immersion objective-lens, NA = 1.3). Red lines that are superimposed in each image denote our length measurements for each DNA strand. Scale bar, $10\ \mu\text{m}$. (c) DNA length measurement results of our mobile phone device plotted against the benchtop microscope results. Each one of these DNA molecules ($N = 236$) reported in this curve has been imaged by both our mobile phone microscope and a benchtop fluorescence microscope, providing a one-to-one comparison between the two platforms. The red curve is a linear fit to the raw data. (d) The distribution of the length measurement differences (Δl) between mobile phone and microscope results, where the mean error is $-0.33\ \mu\text{m}$ and the standard deviation is $1.08\ \mu\text{m}$.

fact that red and blue pixels of the raw Bayer pattern are not used in our analysis (Figure 3c). The next step is the generation of an object mask (see Figure 3d) for each DNA molecule, which is automatically implemented by using a curvature detection algorithm to isolate the junctions of overlapping regions/masks due to closely located DNA molecules, significantly improving the overall detection efficiency of DNA strands (see Figure S3 and the Supporting Information). The fourth step of our algorithm is to find the skeleton (blue line in Figure 3e) of each DNA molecule through PSF fitting. The PSF of our cellphone microscope was estimated by averaging the 2D intensity profiles of 100 nm fluorescent particles imaged on the same mobile device. The PSF fitting procedure is initially applied to the short axis of each DNA molecule to find its center. Note that this fitting process cannot be as accurate as determining the lateral position of a single fluorescent molecule since (1) our PSF is estimated using 100 nm particles, and (2) there are more than one fluorescent molecule along the short-axis of each DNA strand; however, this does not pose a limitation for our current mobile microscopy design and would be important to consider only for platforms that can achieve much smaller sizing accuracy and precision. Then, the peak points of

these centers are connected to form a DNA skeleton along the long axis direction. The next step is to find the edges of the DNA strand along its long axis by comparing a PSF-based theoretical edge intensity profile with the measured intensity profile of the cellphone image (Figure 3f). The PSF-based edge function is digitally slided on the DNA skeleton toward both of its ends until a minimum difference between the theoretical and the actual edge functions was observed. The estimated length of the stretched DNA molecule is then indicated by a red curve that connects both of these end points through the calculated skeleton (see, e.g., the red string in Figure 3g). For extremely low SNR DNA molecules, where these PSF fitting procedures cannot be successfully applied, the length of the molecule can also be estimated by thresholding the measured DNA intensity profile.

To test the accuracy and precision of our cellphone-based DNA length measurements, we used a conventional benchtop fluorescence microscope with a $100\times$ oil-immersion objective lens (NA = 1.3) and a passively cooled CCD camera as our reference method. Figure 4a,b display zoomed-in regions of the λ DNA sample imaged on our mobile phone platform and a conventional fluorescence microscope, respectively,

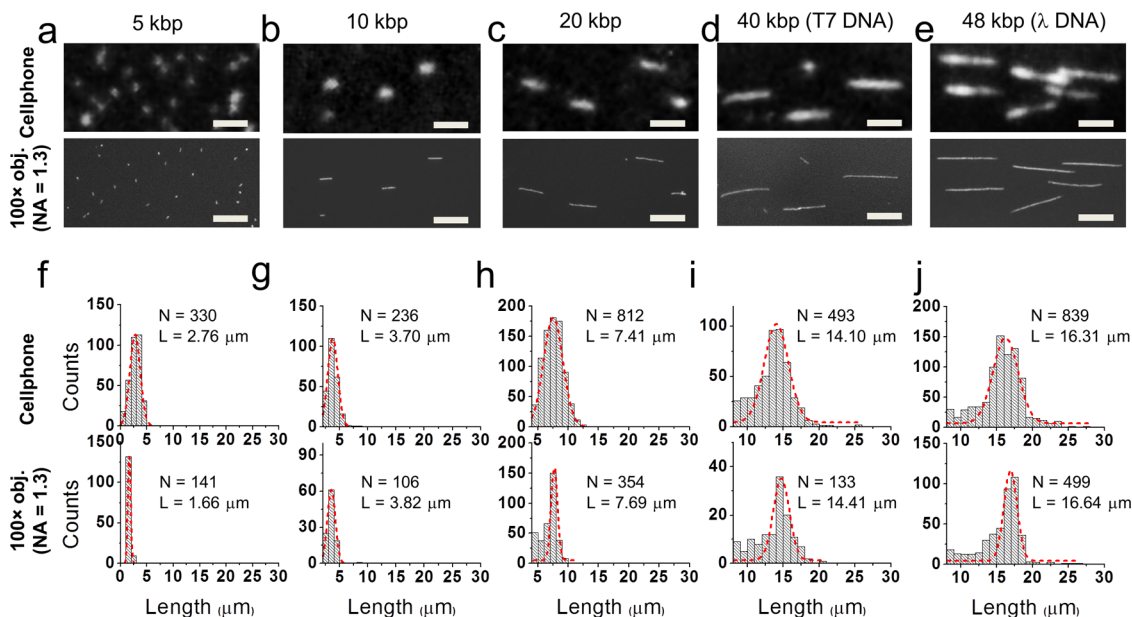


Figure 5. Length measurements of individual DNA molecules. (a–e) Cellphone images (top row) and benchtop fluorescence microscope images ($100\times$ obj., NA = 1.3) (second row) of 5, 10, 20, 40, and 48 kbp DNA samples, respectively. Scale bars, $10\ \mu\text{m}$. (f–j) Length histograms of single DNA molecules measured using our cellphone device (third row) and a benchtop fluorescence microscope (bottom row), respectively. The average DNA length (L) for each histogram is calculated by automatically fitting a Gaussian, *i.e.*, a normal distribution, and taking the mean of the fitted function (shown with the dashed curve for each histogram).

and each DNA molecule image is superimposed with a length profile (red line) calculated using the computational procedures outlined earlier. As illustrated in Figure 4c, DNA length values measured on our cellphone platform are in decent agreement with those obtained using the benchtop fluorescence microscope. The mean error for our cellphone based length measurement results is $\sim 0.33\ \mu\text{m}$ or $\sim 0.96\ \text{kbp}$ (shorter) compared to benchtop microscope measurements, with a standard deviation of $\sim 1.08\ \mu\text{m}$ or $\sim 3.17\ \text{kbp}$ (Figure 4d).

We also performed experiments for differentiating five different DNA sequences that are combed, imaged, and measured under the same imaging conditions by using our cellphone microscopy platform (see Figures 5 and 6). In these experiments, we selected relatively large molecular weight DNA strands, corresponding to 48.5 kbp (λ DNA) and 39.9 kbp (T7 DNA), where conventional gel electrophoresis methods would not be able to differentiate (see, *e.g.*, Figure S4), as well as three shorter DNA fragments (5, 10, and 20 kbp) to demonstrate a broad sizing range (Figure 6). Figure 5a–e show these single DNA molecules with various lengths imaged by our cellphone microscope (top row) and a benchtop inverted fluorescence microscope equipped with a $100\times$ objective lens (NA = 1.3) and a cooled monochrome CCD camera (second row). Figure 5f–j illustrate the length distributions of these DNA samples quantified by our cellphone based imaging platform as well as the conventional fluorescence microscope. The measured number of DNA molecules

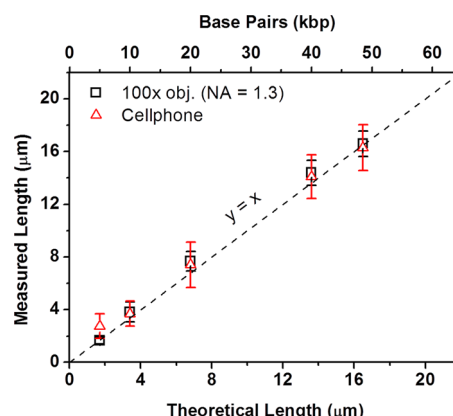


Figure 6. Comparison of the mean DNA lengths measured by the cellphone (red triangle) and benchtop fluorescence microscope (black square). Theoretical length of the fully stretched DNA molecule was calculated based on $0.34\ \text{nm}$ per base pair. The full length of the error bar for each data point represents twice the standard deviation of a normal distribution curve that is fitted to the measured DNA length histograms shown in Figure 5f–j.

(N) is significantly less in benchtop microscope measurements compared to our mobile phone results due to much smaller FOV of the $100\times$ objective lens (see, *e.g.*, Figure 2a). The average lengths (L) of the stretched λ and T7 DNA molecules (Figure 5i,j) measured using our cellphone were 16.31 and $14.10\ \mu\text{m}$, respectively, which were in good agreement with 16.64 and $14.41\ \mu\text{m}$ that were measured using the conventional benchtop microscope, yielding an average length measurement accuracy of 98.0 and 97.8% , respectively. We should

reemphasize that separation and detection of large molecular weight DNA segments are major challenges for conventional gel electrophoresis techniques, which work better for small DNA fragments as also illustrated in Figure S4.

This decent agreement in our measurement results was also observed on shorter DNA fragments (20 and 10 kbp) as illustrated in Figure 5g,h and Figure 6, yielding an average length measurement accuracy of 96.4 and 96.9% for 20 and 10 kbp DNA samples, respectively, compared to the benchtop microscope measurements. These results, as summarized in Figures 5 and 6, illustrate that for 10 kbp and longer DNA molecules our mobile phone platform can achieve an average DNA sizing accuracy of $<0.34\text{ }\mu\text{m}$ or $<1\text{ kbp}$. On the other hand, for 5 kbp DNA samples, the average length measured by our mobile phone based imaging platform was considerably longer compared to the benchtop microscope measurement results as illustrated in Figure 5f ($L = 2.76\text{ }\mu\text{m}$ vs $L = 1.66\text{ }\mu\text{m}$, respectively). This length measurement discrepancy for 5 kbp DNA samples can be attributed to our reduced detection SNR for such short DNA fragments as well as to the limited spatial resolution of our mobile phone, both of which can be substantially improved by, *e.g.*, substituting the current external lens in our imaging design with a higher numerical aperture lens. Further improvements in our image quality and sizing accuracy can also be achieved by using specially designed substrates, including for example plasmonic metal films or nanostructure arrays, to significantly

increase the fluorescent signal of each DNA molecule through field enhancements.

CONCLUSIONS

In conclusion, we reported the first demonstration of imaging and sizing of individual DNA molecules on a mobile phone microscope. This simple, field-portable, and cost-effective fluorescent microscopy platform installed on a mobile phone permits direct visualization of individual DNA molecules that are fluorescently labeled over a large FOV of $\sim 2\text{ mm}^2$. A robust image processing framework that is integrated with the cloud was also developed to overcome the SNR challenge and allow quantitative length measurements of single DNA molecules imaged on our mobile phone platform, achieving a sizing accuracy of $<1\text{ kbp}$ for 10 kbp and longer DNA samples. This mobile phone based imaging platform provides a unique solution for sizing of DNA molecules and might also be utilized for determining CNVs in genome using a field-portable and cost-effective design, a distinct capability that can be broadly used in various clinical applications including for example the detection of cancers (*e.g.*, stomach, brain, *etc.*), nervous system disorders or even drug resistance in infectious diseases. Offering spatiotemporal data mapping, this single molecule DNA imaging and sizing platform could also assist, *e.g.*, health-care professional, epidemiologists and policy makers, among others, to track emerging trends and shed more light on genetic cause-effect relationships in point-of-care and resource limited settings.

METHODS

Design of Cellphone-Integrated Fluorescence Microscopy. A field-portable cellphone-based fluorescence microscope was created by integrating a 3D printed optomechanical attachment to the existing camera module of a smartphone (Lumia 1020, Nokia). This robust cellphone attachment was designed in Autodesk Inventor and printed by using a 3D printer (Dimension Elite 3D). A 450 nm laser diode powered by three AAA batteries and a constant current output driver was used as the excitation light, which illuminated the sample at an incidence angle of $\sim 75^\circ$. The laser beam was focused through a small convex lens ($f = 35\text{ mm}$) to form a tight illumination spot. The average illumination power density at the sample plane was estimated to be 2.4 W/cm^2 . To dissipate the heat, the laser diode was mounted on a $\Phi 12 \times 30\text{ mm}$ copper host and further surrounded by a $\Phi 18 \times 40\text{ mm}$ aluminum heatsink. The focus of the cellphone microscope was controlled by a miniature dovetail stage (DT12, Thorlabs) which moved both the sample chamber and the light source. The fluorescence signal emitted from the specimen was collected through an external lens ($f = 4\text{ mm}$) in addition to the built-in cellphone camera lens ($f = 6.5\text{ mm}$), and finally recorded by the cellphone CMOS sensor chip (pixel pitch: $1.12\text{ }\mu\text{m}$; image size: 7152×5368 pixels). Two stacked 500 nm long-pass filters (FF01-500/LP-23.3-D, Semrock) were placed between the external lens and the cellphone camera lens to reject the scattered background light due to high-power laser excitation.

Fluorescence Labeling and Stretching of DNA Molecules. DNA fragments (5, 10, and 20 kbp, Thermo Scientific), Lambda DNA

(48,502 bp, Life Technologies) and T7 DNA (39,937 bp, Boca Scientific Inc.) were labeled with an intercalating dye YOYO-1 (Excitation/Emission = 491/509 nm, Life Technologies) at a base pair to dye molecule ratio of 5:1 following a standard labeling protocol (see Supporting Information).

Before stretching of DNA molecules, prestained DNA solutions were warmed up at 65°C for 10 min, followed by a quick cooling in running water for 2 min to open up the sticky ends of DNA. Then, $5\text{ }\mu\text{L}$ of this prelabeled DNA solution was diluted in $110\text{ }\mu\text{L}$ imaging buffer ($1 \times$ TAE buffer added with 4.8% (v/v) 2-mercaptoethanol and 500 nm green fluorescent beads) to a final concentration of $\sim 0.03\text{ ng}/\mu\text{L}$.

To stretch DNA molecules using a simple and rapid method,⁴⁸ a $22 \times 22\text{ mm}$ silanized coverslip (see Supporting Information) was placed on a solid planar surface, and $3\text{ }\mu\text{L}$ of the stained DNA solution diluted in imaging buffer was pipetted onto the center of the coverslip. Another $18 \times 18\text{ mm}$ plasma-treated coverslip was held horizontally which was approximately 1 mm above the bottom coverslip. The top coverslip was then quickly pressed down toward the bottom substrate with a tweezer. The droplet containing the DNA samples was pushed from the center to the edges between the top and bottom coverslips, forming a strong shearing flow, which stretches the DNA molecules on the bottom substrate. The sample was then sealed with colorless nail polish and imaged using our microscopes.

Image Acquisition. The DNA sample of interest, after the preparation steps detailed earlier, was loaded onto our sample holder and inserted into the cellphone attachment. All the fluorescence images were recorded in a lossless raw format

(DNG) with an integration time of ~4 s per frame. About 10–15 frames of the same DNA sample were captured for image averaging, before photobleaching was observed.

Windows Based Smart Mobile Application Development. We created a custom-developed Windows phone application that allows for analysis of the lengths of single DNA molecules imaged on the phone (see Figure 1a and Figure S5). This application can be used to capture an image of the sample or alternatively open a saved image for DNA length measurement (Figure S5a,b). The selected or captured image is subsequently uploaded to a remote server through HTTP for rapid digital processing (Figure S5c). On this server, the uploaded image is first converted from DNG format to 16-bit TIFF format and then processed in MATLAB using the length quantification method described previously (Figure 3). Once the processing is finished (Figure S5d), the results (a histogram of DNA length measurements and a corresponding labeled image marking all the locations of analyzed DNA molecules) are then sent back to the originating phone (Figure S5e,f). The processing time for a 200 × 200 pixel cropped section of the full field-of-view is ~7 s in MATLAB using a single PC (CPU: Intel Xeon E5–2620), and it can be reduced by more than an order of magnitude if the same algorithms are implemented in a more efficient software language such as C/C++ and/or adapted to utilize GPUs. Depending on the network speed, the upload time of the 41 megapixel raw DNG image varies between 10 s to 3 min.

Conflict of Interest: The authors declare the following competing financial interest(s): A. Ozcan is the co-founder of a start-up company that aims to commercialize computational microscopy tools.

Acknowledgment. This project was funded by an EAGER Award from NSF (National Science Foundation). Ozcan Research Group at UCLA gratefully acknowledges the support of the Presidential Early Career Award for Scientists and Engineers (PECASE), Army Research Office (ARO; W911NF-13-1-0419 and W911NF-13-1-0197), ARO Life Sciences Division, NSF CAREER Award, NSF CBET Division Biophotonics Program, NSF Emerging Frontiers in Research and Innovation (EFRI) Award, Office of Naval Research (ONR) and the Howard Hughes Medical Institute (HHMI). This work is based upon research performed in a renovated laboratory by the National Science Foundation under Grant No. 0963183, which is an award funded under the American Recovery and Reinvestment Act of 2009 (ARRA). H.O. also acknowledges the partial support of TUBITAK (The Scientific and Technological Research Council of Turkey) and the Fatih Sultan Mehmet Vakif University in Turkey.

Supporting Information Available: Supporting methods and figures. This material is available free of charge via the Internet at <http://pubs.acs.org>.

REFERENCES AND NOTES

- Yildiz, A.; Forkey, J. N.; McKinney, S. A.; Ha, T.; Goldman, Y. E.; Selvin, P. R. Myosin V Walks Hand-over-Hand: Single Fluorophore Imaging with 1.5-nm Localization. *Science* **2003**, *300*, 2061–2065.
- Schwartz, J. J.; Quake, S. R. Single Molecule Measurement of The “Speed Limit” of DNA Polymerase. *Proc. Natl. Acad. Sci. U. S. A.* **2009**, *106*, 20294–20299.
- Harris, T. D.; Buzby, P. R.; Babcock, H.; Beer, E.; Bowers, J.; Braslavsky, I.; Causey, M.; Colonell, J.; DiMeo, J.; Efcaivitch, J. W.; et al. Single-Molecule DNA Sequencing of a Viral Genome. *Science* **2008**, *320*, 106–109.
- Greenleaf, W. J.; Woodside, M. T.; Block, S. M. High-Resolution, Single-Molecule Measurements of Biomolecular Motion. *Annu. Rev. Biophys. Biomol. Struct.* **2007**, *36*, 171–190.
- Cisse, I.; Okumus, B.; Joo, C.; Ha, T. Fueling Protein-DNA Interactions inside Porous Nanocontainers. *Proc. Natl. Acad. Sci. U. S. A.* **2007**, *104*, 12646–12650.
- Seisenberger, G.; Ried, M. U.; Endreß, T.; Büning, H.; Hallek, M.; Bräuchle, C. Real-Time Single-Molecule Imaging of the Infection Pathway of an Adeno-Associated Virus. *Science* **2001**, *294*, 1929–1932.
- Moerner, W. E. New Directions in Single-Molecule Imaging and Analysis. *Proc. Natl. Acad. Sci. U. S. A.* **2007**, *104*, 12596–12602.
- Tokunaga, M.; Imamoto, N.; Sakata-Sogawa, K. Highly Inclined Thin Illumination Enables Clear Single-Molecule Imaging in Cells. *Nat. Methods* **2008**, *5*, 159–161.
- Ha, T.; Enderle, T.; Chemla, D. S.; Selvin, P. R.; Weiss, S. Single Molecule Dynamics Studied by Polarization Modulation. *Phys. Rev. Lett.* **1996**, *77*, 3979–3982.
- Rust, M. J.; Bates, M.; Zhuang, X. Sub-Diffraction-Limit Imaging by Stochastic Optical Reconstruction Microscopy (STORM). *Nat. Methods* **2006**, *3*, 793–796.
- Betzig, E.; Patterson, G. H.; Sougrat, R.; Lindwasser, O. W.; Olenych, S.; Bonifacino, J. S.; Davidson, M. W.; Lippincott-Schwartz, J.; Hess, H. F. Imaging Intracellular Fluorescent Proteins at Nanometer Resolution. *Science* **2006**, *313*, 1642–1645.
- Chou, H.-P.; Spence, C.; Scherer, A.; Quake, S. A Microfabricated Device for Sizing and Sorting DNA Molecules. *Proc. Natl. Acad. Sci. U. S. A.* **1999**, *96*, 11–13.
- Pertsinidis, A.; Zhang, Y.; Chu, S. Subnanometre Single-Molecule Localization, Registration and Distance Measurements. *Nature* **2010**, *466*, 647–651.
- Stankiewicz, P.; Lupski, J. R. Structural Variation in the Human Genome and Its Role in Disease. *Annu. Rev. Med.* **2010**, *61*, 437–455.
- Lee, J. A.; Lupski, J. R. Genomic Rearrangements and Gene Copy-Number Alterations as a Cause of Nervous System Disorders. *Neuron* **2006**, *52*, 103–121.
- Forget, A. L.; Kowalczykowski, S. C. Single-Molecule Imaging of DNA Pairing by RecA Reveals a Three-Dimensional Homology Search. *Nature* **2012**, *482*, 423–427.
- Teague, B.; Waterman, M. S.; Goldstein, S.; Potamousis, K.; Zhou, S.; Reslewic, S.; Sarkar, D.; Valouev, A.; Churas, C.; Kidd, J. M.; et al. High-Resolution Human Genome Structure by Single-Molecule Analysis. *Proc. Natl. Acad. Sci. U. S. A.* **2010**, *107*, 10848–10853.
- Sidorova, J. M.; Li, N.; Schwartz, D. C.; Folch, A.; Monnat, R. J., Jr. Microfluidic-Assisted Analysis of Replicating DNA Molecules. *Nat. Protocols* **2009**, *4*, 849–861.
- Baday, M.; Cravens, A.; Hastie, A.; Kim, H.; Kudeki, D. E.; Kwok, P.-Y.; Xiao, M.; Selvin, P. R. Multicolor Super-Resolution DNA Imaging for Genetic Analysis. *Nano Lett.* **2012**, *12*, 3861–3866.
- Yu, H.; Shan, X.; Wang, S.; Chen, H.; Tao, N. Plasmonic Imaging and Detection of Single DNA Molecules. *ACS Nano* **2014**, *8*, 3427–3433.
- Ozcan, A. Mobile Phones Democratize and Cultivate Next-Generation Imaging, Diagnostics and Measurement Tools. *Lab Chip* **2014**, *14*, 3187–3194.
- Vashist, S.; Mudanyali, O.; Schneider, E. M.; Zengerle, R.; Ozcan, A. Cellphone-Based Devices for Bioanalytical Sciences. *Anal. Bioanal. Chem.* **2014**, *406*, 3263–3277.
- Ozcan, A. Educational Games for Malaria Diagnosis. *Sci. Transl. Med.* **2014**, *6*, 233ed9.
- Mudanyali, O.; Dimitrov, S.; Sikora, U.; Padmanabhan, S.; Navruz, I.; Ozcan, A. Integrated Rapid-Diagnostic-Test Reader Platform on a Cellphone. *Lab Chip* **2012**, *12*, 2678–2686.
- Zhu, H.; Sikora, U.; Ozcan, A. Quantum Dot Enabled Detection of *Escherichia coli* Using a Cell-Phone. *Analyst* **2012**, *137*, 2541–2544.
- Coskun, A. F.; Wong, J.; Khodadadi, D.; Nagi, R.; Tey, A.; Ozcan, A. A Personalized Food Allergen Testing Platform on a Cellphone. *Lab Chip* **2013**, *13*, 636–640.
- Wei, Q.; Qi, H.; Luo, W.; Tseng, D.; Ki, S. J.; Wan, Z.; Göröcs, Z.; Bentolila, L. A.; Wu, T.-T.; Sun, R.; et al. Fluorescent Imaging of Single Nanoparticles and Viruses on a Smart Phone. *ACS Nano* **2013**, *7*, 9147–9155.
- Feng, S.; Caire, R.; Cortazar, B.; Turan, M.; Wong, A.; Ozcan, A. Immunochromatographic Diagnostic Test Analysis Using Google Glass. *ACS Nano* **2014**, *8*, 3069–3079.
- Filippini, D.; Alimelli, A.; Di Natale, C.; Paolesse, R.; D’Amico, A.; Lundström, I. Chemical Sensing with Familiar Devices. *Angew. Chem., Int. Ed.* **2006**, *45*, 3800–3803.

30. Won, B. Y.; Park, H. G. A Touchscreen as a Biomolecule Detection Platform. *Angew. Chem., Int. Ed.* **2012**, *51*, 748–751.
31. Breslauer, D. N.; Maamari, R. N.; Switz, N. A.; Lam, W. A.; Fletcher, D. A. Mobile Phone Based Clinical Microscopy for Global Health Applications. *PLoS One* **2009**, *4*, e6320.
32. Martinez, A. W.; Phillips, S. T.; Whitesides, G. M.; Carrilho, E. Diagnostics for the Developing World: Microfluidic Paper-Based Analytical Devices. *Anal. Chem.* **2009**, *82*, 3–10.
33. Smith, Z. J.; Chu, K.; Wachsmann-Hogiu, S. Nanometer-Scale Sizing Accuracy of Particle Suspensions on an Unmodified Cell Phone Using Elastic Light Scattering. *PLoS One* **2012**, *7*, e46030.
34. Oncescu, V.; O'Dell, D.; Erickson, D. Smartphone Based Health Accessory for Colorimetric Detection of Biomarkers in Sweat and Saliva. *Lab Chip* **2013**, *13*, 3232–3238.
35. Oncescu, V.; Mancuso, M.; Erickson, D. Cholesterol Testing on a Smartphone. *Lab Chip* **2014**, *14*, 759–763.
36. Gallegos, D.; Long, K. D.; Yu, H.; Clark, P. P.; Lin, Y.; George, S.; Nath, P.; Cunningham, B. T. Label-Free Biodection Using a Smartphone. *Lab Chip* **2013**, *13*, 2124–2132.
37. Pamplona, V. F.; Mohan, A.; Oliveira, M. M.; Raskar, R. NETRA: Interactive Display for Estimating Refractive Errors and Focal Range. *ACM Trans. Graphics* **2010**, *29*, 77.
38. Haun, J. B.; Castro, C. M.; Wang, R.; Peterson, V. M.; Marinelli, B. S.; Lee, H.; Weissleder, R. Micro-NMR for Rapid Molecular Analysis of Human Tumor Samples. *Sci. Transl. Med.* **2011**, *3*, 71ra16.
39. Shen, L.; Hagen, J. A.; Papautsky, I. Point-of-Care Colorimetric Detection with a Smartphone. *Lab Chip* **2012**, *12*, 4240–4243.
40. Zhu, H.; Mavandadi, S.; Coskun, A. F.; Yaglidere, O.; Ozcan, A. Optofluidic Fluorescent Imaging Cytometry on a Cell Phone. *Anal. Chem.* **2011**, *83*, 6641–6647.
41. Zhu, H.; Sencan, I.; Wong, J.; Dimitrov, S.; Tseng, D.; Nagashima, K.; Ozcan, A. Cost-Effective and Rapid Blood Analysis on a Cell-Phone. *Lab Chip* **2013**, *13*, 1282–1288.
42. Coskun, A. F.; Nagi, R.; Sadeghi, K.; Phillips, S.; Ozcan, A. Albumin Testing in Urine Using a Smart-Phone. *Lab Chip* **2013**, *13*, 4231–4238.
43. Wei, Q.; Nagi, R.; Sadeghi, K.; Feng, S.; Yan, E.; Ki, S. J.; Caire, R.; Tseng, D.; Ozcan, A. Detection and Spatial Mapping of Mercury Contamination in Water Samples Using a Smart-Phone. *ACS Nano* **2014**, *8*, 1121–1129.
44. Ludwig, S. J.; Zhu, H.; Phillips, S.; Shiledar, A.; Feng, S.; Tseng, D.; van Ginkel, L.; Nielan, M. F.; Ozcan, A. Cellphone-Based Detection Platform for Rbst Biomarker Analysis in Milk Extracts Using a Microsphere Fluorescence Immunoassay. *Anal. Bioanal. Chem.* **2014**, *406*, 6857–6866.
45. Ray, M.; Goldstein, S.; Zhou, S.; Potamousis, K.; Sarkar, D.; Newton, M. A.; Esterberg, E.; Kendziora, C.; Bogler, O.; Schwartz, D. C. Discovery of Structural Alterations in Solid Tumor Oligodendroglioma by Single Molecule Analysis. *BMC Genomics* **2013**, *14*, 505.
46. Herrick, J.; Michalet, X.; Conti, C.; Schurra, C.; Bensimon, A. Quantifying Single Gene Copy Number by Measuring Fluorescent Probe Lengths on Combed Genomic DNA. *Proc. Natl. Acad. Sci. U. S. A.* **2000**, *97*, 222–227.
47. Price, R. N.; Uhlemann, A.-C.; Brockman, A.; McGready, R.; Ashley, E.; Phaipun, L.; Patel, R.; Laing, K.; Looareesuwan, S.; White, N. J.; et al. Mefloquine Resistance in *Plasmodium falciparum* and Increased *pfdmfr1* Gene Copy Number. *Lancet* **2004**, *364*, 438–447.
48. Chan, T.-F.; Ha, C.; Phong, A.; Cai, D.; Wan, E.; Leung, L.; Kwok, P.-Y.; Xiao, M. A Simple DNA Stretching Method for Fluorescence Imaging of Single DNA Molecules. *Nucleic Acids Res.* **2006**, *34*, e113.
49. Adobe Photoshop: Digital Negative (DNG). <http://helpx.adobe.com/photoshop/digital-negative.html>. Accessed Dec 10, 2014.
50. Bayer, B. E., Color Imaging Array. U.S. Patent 3,971,065, Jul 20, 2005.